Time-Domain Relay Performance Evaluation Considering Brazilian Fault Cases

Felipe V. Lopes, João Paulo G. Ribeiro, Tiago R. Honorato, Kleber M. Silva, Joaquim Neto Rezende Jr., Carlos A. M. Aviz, Rafael O. Fernandes

***Abstract*—This paper presents the performance evaluation of an actual time-domain transmission line protective relay. This kind of study has been requested by Brazilian utilities to better clarify questions on the SEL-T400L relay performance, which is a commercially available time-domain protective device, whose concepts are still somewhat new to Brazilian protection engineers. SEL-T400L belongs to a new generation of high-speed microprocessed relays which overcome the need for phasor estimation, thereby it is faster than traditional phasor-based devices. To perform the proposed evaluation, playback tests using actual SEL-T400L relays were carried out, considering real-world and simulated fault scenarios in a 230 kV/60 Hz Brazilian transmission line with high number of outages per year. The results demonstrate that the SEL-T400L relay is indeed able to operate in times of the order of few milliseconds for internal faults, without loss of security in external fault cases. In the analyzed scenarios, it proved to be one power cycle faster than the phasor-based relays currently installed in the evaluated system.**

***Keywords*—Brazilian power grid, SEL-T400L, time-domain protection, transmission lines, power systems.**

I. Introduction

In recent years, transmission line protection schemes have evolved from stand-alone phasor-based protective devices to time-domain relays with high sampling rates and high speed communication schemes. Such a new generation of relays results from the need to provide fast fault identification in heavy loaded transmission networks, which operate close to their stability limits [1]. Indeed, time-domain relays have shown to be able to reduce the protection operation times in relation to traditional phasor-based relays, resulting in larger system stability margins, without compromising the protection schemes security.

In the context of time-domain transmission line protective devices, the SEL-T400L relay has attracted the attention of several utilities worldwide [2]. It has four main time-domain protection elements, namely: TD21 (incremental quantity-based distance protection), TD32 (incremental quantity-based directional protection), TW32 (traveling wave-based directional protection) and TW87 (traveling wave-based differential protection). These functions also rely on other auxiliary protection functions, such as the directional and non-directional time-domain overcurrent elements OC21, OCTP and OC87, which supervise the operation of TD21, TD32/TW32 and TW87, respectively, guaranteeing the relay dependability during non-fault disturbances that may generate transients [2]. As reported in [3], the SEL-T400L average operation time is of about 4 ms, but tripping times of the order of 1 ms can be verified, depending on the system topology, size and operation conditions.

Although SEL-T400L has shown to be promising for real-world systems, as reported in [3], its main principles and some performance issues are still somewhat new for protection engineers. In [4] and [5], several fault scenarios were simulated to test the SEL-T400L functions. However, although the analyzed tests clarify some questions regarding the performance of time-domain protection functions, the results were obtained from a computational relay model, considering only simulated cases. Therefore, utilities have demonstrated an increasingly interest for researches that demonstrate the time-domain relay performance in real-world fault cases, with results taken from actual devices. In this context, from the authors' best knowledge, only the SEL-T400L manufacturer has reported results obtained from actual fault scenarios by using real time-domain relays [3], so that Brazilian protection engineers have requested further SEL-T400L studies, specially to better understand what would be its performance if applied in the Brazilian interconnected transmission network.

In order to respond to the aforementioned demand, this paper evaluates the SEL-T400L performance considering Brazilian fault cases in a transmission line with high number of outages per year. Firstly, real records are taken to analyze the TD21 and TD32 performances, comparing their operation times with those obtained from the phasor-based relays in the field. Then, a realistic model of the evaluated system is simulated using the Alternative Transients Program (ATP) to analyze cases in which the TD21, TD32, TW32 and TW87 operate together. All studied tests are performed using actual SEL-T400L relays, whose input signals were generated by means of appropriate test sets and relay functionalities. The obtained results show that the SEL-T400L relay is promising for the evaluated line, being able to quickly operate in internal fault cases, and being secure during external disturbances.

This work was supported by the Brazilian National Research Council (CNPq) and Coordination for the Improvement of Higher Education Personnel (CAPES).

Felipe Lopes, João Paulo, Tiago Honorato and Kleber Silva are with the Department of Electrical Engineering at University of Brasília (UnB), 70910-900 Brasília-DF, Brazil. (e-mail: felipevlopes@ene.unb.br, joaopaulogribeiro@gmail.com, tiagohonorato1@gmail.com, klebermelo@unb.br).

Joaquim Rezende Jr. is with Eletronorte, Brasília, Brazil (e-mail: joaquim.junior@eletronorte.gov.br).

Carlos Aviz is with Aviz Consultoria, Brasília, Brazil (e-mail: camaaviz@gmail.com).

Rafael Fernandes is with the Transmission System Operator (ONS), Brasília, Brazil (e-mail: rafael.fernandes@ons.org.br).

Paper submitted to the International Conference on Power Systems Transients (IPST2019) in Perpignan, France, June 17-20, 2019.

II. SEL-T400L Principles

As mentioned earlier, SEL-T400L relay has four time-domain protection functions, being two of them based on incremental quantities (TD32 and TD21), and the other two based on traveling waves (TW32 and TW87). As this paper focuses on the SEL-T400L performance analysis considering Brazilian fault cases, the main operation principles of these functions are only briefly described in this section, but further details can be found in [2].

A. Incremantal Quantity-Based Functions

The directional element TD32 and the distance element TD21 are the incremental quantity-based functions available in SEL-T400L. Both use a current signal immune to decaying dc component, called incremental replica current (Δi_z), which compensates phase displacements caused by the inductive line characteristic, but maintaining an unitary gain. As a result, zero-crossings of voltages and incremental replica currents coincide, allowing the amplitude and polarity time-domain analysis of pure fault circuit voltages and currents as if they were taken from a resistive circuit [6].

The TD32 evaluates the operating 'torque' T_{OP}, which carries information on the relative polarity between incremental voltages and currents. Fig. 1 shows a four quadrant plane in which incremental voltage versus incremental current trajectory during internal and external fault cases are illustrated. By using simply the incremental current Δi, the trajectory passes through all the four quadrants. Although it properly indicates the fault direction in the first few instants after the fault inception, such a behavior could jeopardize the protection dependability. On the other hand, when the incremental voltage Δv and the incremental replica current Δi_z are analyzed, the trajectory is narrowed, resulting in well-defined regions for forward and reverse faults, except for the need for a security margin SM. Therefore, considering $T_{OP}(t) = -\Delta v(t) \cdot \Delta i_z(t)$, forward and reverse faults can be distinguished, in such a way that $T_{OP} > 0$ indicate a forward fault (i.e., Δv versus Δi_z trajectory in the second and fourth quadrants), whereas $T_{OP} < 0$ indicate a reverse fault (i.e., Δv versus Δi_z trajectory in the first and third quadrants). Based on that, the TD32 can be implemented using a Permissive Overreach Transfer Trip (POTT) scheme to provide the transmission line unitary protection, whose operation logic also includes the analysis of a non-directional time-domain overcurrent element OCTP to distinguish low energy events from fault cases [2].

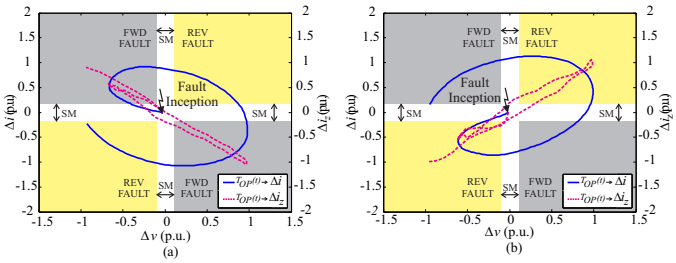

Fig. 1. TD32 operation principle.

Complementing the TD32, the underreach distance element TD21 is used. It analyzes voltage profiles along the faulted line to distinguish in-zone faults from out-of-zone ones. Basically, Δv, Δi_z, as well as prefault voltages and currents are used to estimate operating and restraining voltages at the reaching point m_0, which are called V_{21OP} and V_{21R}, respectively. As the greatest possible voltage variation at the fault point is the prefault voltage V_{PRE}, V_{21R} is obtained based on the the V_{PRE} value, so that the TD21 detects an in-zone fault whether $V_{21OP} \geq V_{21R}$, otherwise, an out-of-zone fault is indicated, as shown in Fig. 2. To avoid false trip during low energy events, a directional overcurrent element OC21 is analyzed. Besides, the TD21 can be applied using a Direct Transfer Trip (DTT) scheme, allowing a quick line tripping even when a single-terminal in-zone fault detection occurs [2].

B. Traveling Wave-Based Functions

The directional element TW32 and the differential element TW87 are the traveling wave-based functions available in SEL-T400L. Both functions use filtered signals taken from the Differentiator-Smoother filter, which responds to typical fault-induced voltage and current step-changes creating triangle-shaped outputs [3], whose peak value is taken as the wavefront amplitude and the instant at which it occurs as the wave arrival time [2].

Aiming to better explain the TW32 and TW87 operation principles, Fig. 3 depicts the Bewley diagram of fault-induced voltage and current traveling waves, called v_{TW} and i_{TW}, respectively, for internal and external fault scenarios, where the Line 2 is taken as the protected line. Considering the polarity of current transformers (CTs) as shown in Fig. 3, it should be observed that currents flowing into the line have relative positive polarity, whereas currents leaving the line have relative negative polarity. Therefore, as shown in Fig. 3(a), in external fault cases, v_{TW} and i_{TW} enter the protected line with the same polarity at the terminal closer to the fault point, whereas they are measured with opposite polarities at

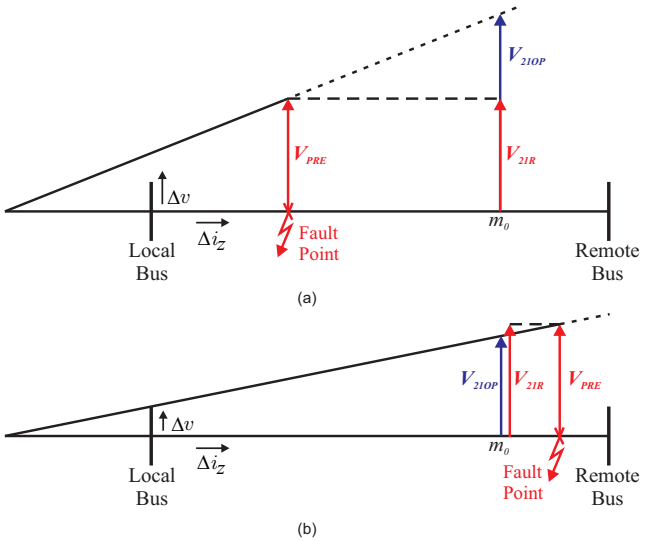

Fig. 2. TD21 operation principle.

the line terminal farthest to the fault point. On the other hand, in internal fault cases, v_{TW} and i_{TW} are measured with the same polarity at both line ends, as illustrated in Fig. 3(b).

Similarly to the TD32, the TW32 calculates an operating 'torque' T_{OP}. Nevertheless, instead of using Δv and Δi_z, the TW32 computes $T_{OP} = -v_{TW} \cdot i_{TW}$, where v_{TW} and i_{TW} stand for the amplitude of the first incident voltage and current traveling waves that reach the monitored terminals, respectively. Thus, positive and negative T_{OP} values are verified in forward and reverse fault cases, respectively, thereby the results obtained from both line terminals can be correlated to distinguish internal from external faults. In SEL-T400L, the TW32 does not trip alone, but rather, it speeds up the POTT scheme by interacting with the TD32. By doing so, if the TD32 detects a forward fault in a given terminal, and the TW32 detects also a forward fault at the opposite line end, a high-speed permissive trip signal is issued to accelerate the POTT operation.

Fig. 3 can be also used to explain the TW87 principles. Unlike traditional phasor-based differential schemes, the TW87 compares the amplitudes of traveling waves, considering polarity and arrival time information taken from both line ends [3]. In addition to the already explained polarity relations of fault-induced waves that enter and leave the monitored line, one should note that, in external fault cases, current waves that reach a given line terminal leave the line at the opposite side after the line propagation time τ. On the other hand, for internal faults, the first i_{TW} at both line terminals are of matching polarity and their arrival time difference P is smaller than τ. Based on that, operating and restraining signals called $i_{OP}(t)$ and $i_{RT}(t)$ respectively are defined, being: $i_{OP}(t) = |i_{TWR}(t) + i_{TWL}(t - P)|$ and $i_{RT}(t) = |i_{TWR}(t) - i_{TWL}(t - \tau)|$, where i_{TWL} and i_{TWR} stand for the traveling waves extracted from the local and remote line terminals, respectively. Hence, for external faults, assuming a lossless line, i_{OP} is ideally zero whereas i_{RT} presents large values. On the other hand, for internal faults, $i_{OP}(t) > S \cdot i_{RT}(t)$, where S is a restraining factor. Finally, it is noteworthy to point out that the TW87 also counts with an auxiliary security layers, among which a non-directional overcurrent element OC87 is used to distinguish faults from other events that launch traveling waves on the line.

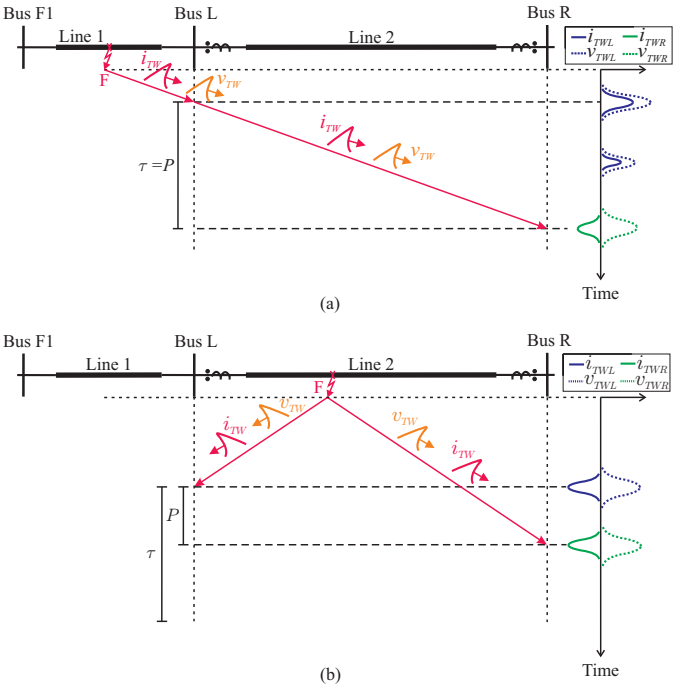

Fig. 3. TW32 and TW87 operation principle.

III. Test System and Relay Testing Methodology

To provide a robust evaluation of SEL-T400L protection functions, an actual 230 kV/60 Hz transmission system with high number of outages per year was chosen (more than forty outages from 2014 to 2015), which is currently equipped with phasor-based protective devices of different manufacturers, whose brands are omitted due to confidentiality reasons.

Fig. 4 shows the test system. It consists of a triple-circuit line 343 km long that connects the Jauru substation (JAU) to the Vilhena substation (VIL), which are located in Mato Grosso and Rondônia states in Brazil, respectively. The analyzed fault records were taken from protective relays installed at both terminals of the line-circuit C3, which belongs to Eletronorte, currently considered one of the biggest Brazilian utilities. Simulated records were also generated by using the ATP software, through which the test power system was modeled, considering the actual electrical parameters provided by Eletronorte and Brazilian Transmission System Operator (ONS). To analyze both actual and simulated records, real SEL-T400L relays were used, whose settings were derived following the instructions reported in [7]. Table I presents the applied settings, where TD32ZF and TD32ZR are the TD32 forward and reverse fault impedance thresholds, respectively, TD21MP and TD21MG are the TD21 phase and ground element reach, respectively, TWLPT is the line propagation time, EXTSC is the external series compensation flag, TP67P and TP67G are the phase and ground OCTP thresholds, respectively, TP50P and TP50G are the phase and ground OC87 thresholds, respectively, Z1MAG∠Z1ANG and Z0MAG∠Z0ANG are the polar representation of positive and zero sequence line impedance, respectively, and PTR and CTR are the potential transformer (PT) and CT ratios [2].

The time-domain relay evaluation is divided into two parts. Firstly, real-world fault records were analyzed. Since these records have a limited sampling rate (maximum of 256 samples/cycle), only the TD32 and TD21 functions were evaluated. A total of 8 real-world fault cases were tested by using a Doble F6150-SV test set to playback the records in the SEL-T400L relays [8]. Then, in the second evaluation part, ATP simulated fault records with sampling rates equal to 1 MHz were analyzed, making it possible to analyze the simultaneous operation of incremental quantity- and traveling wave-based functions. As the Doble F6150-SV test set is not able to reproduce frequencies in the order of hundreds of kilohertz, in this evaluation part, the SEL-T400L playback function was used [9].

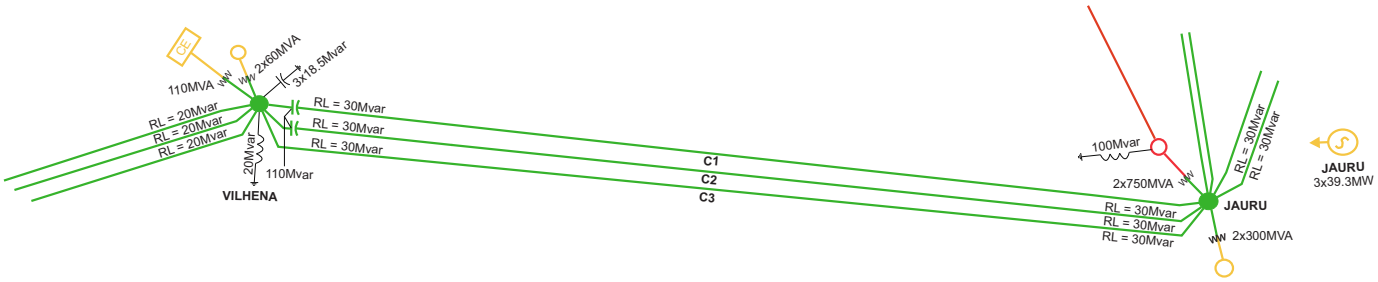

Fig. 4. Test power system: 230 kV/60 Hz JAU-VIL transmission line.

TABLE I
TIME-DOMAIN RELAY USER-DEFINED SETTINGS AND LINE PARAMETERS.

Relay function	**Setting name**	**Setting value in VIL / JAU**
TD32*	TD32ZF	1.16 Ω_{sec} / 0.66 Ω_{sec}
	TD32ZR	6.12 Ω_{sec} / 6.12 Ω_{sec}
OCTP	TP67P	1.66 A_{sec} / 2.79 A_{sec}
	TP67G	1.52 A_{sec} / 2.06 A_{sec}
TD21**	TD21MP	0.75 p.u. / 0.75 p.u.
	TD21MG	0.70 p.u. / 0.70 p.u.
TW87	TWLPT	1168.7 μs / 1168.7 μs
OC87	TP50P	1.66 A_{sec} / 2.79 A_{sec}
	TP50G	1.52 A_{sec} / 2.06 A_{sec}
TD21 and TW87	EXTSC	NO / YES
Relay function	**Setting name**	**System Parameters**
VIL-JAU line	Z1MAG / Z1ANG	20.41 Ω_{sec} / 82.58°
	Z0MAG / Z0ANG	81.85 Ω_{sec} / 71.83°
PT and CT Ratio	PTR / CTR	2000 / 400

*TW32 accelerates the TD32, but it does not have user-defined settings.

**OC21 element is factory-selected based on the line parameters.

IV. Obtained Results

A. Part 1: TD32 and TD21 Evaluation Using Real-World Fault Records

Table II depicts the results obtained from the first evaluation part, pointing out the analyzed real-world fault features and comparing the operation times of the analyzed SEL-T400L relays and those relays installed in VIL and JAU substations, where PH21 and PH87 stand for the distance and differential phasor-based line protection elements, respectively. In all cases, the fault distance was calculated assuming the VIL substation as the reference.

According to [2], the TD21 and TD32 schemes operate only whether the logic relations (TD21 & OC21) and (TD32 & OCTP) are satisfied. Also, as the TD21 and TD32 can operate under DTT and POTT schemes, respectively, the SEL-T400L operation considering the communication between the relays at VIL and JAU substations is also evaluated in Table III, where a communication link latency equal to 4 ms is taken into account, based on field measurements.

From the presented results, it is demonstrated that the time-domain elements are indeed able to speed up the protection operation by about one power cycle in relation to the phasor-based functions. It should be noted that correct operations were verified in the internal fault cases R1 to R7, as well as in the external fault scenario R8, when the relay restrained the trip, as expected. From Tables II and III, it is observed that the time-domain relay operation times did not exceed 9.8 ms, being such a maximum value obtained in case R2 at both VIL and JAU substations. Furthermore, by analyzing the fastest operations, average operation times of about 3.0 ms and 4.6 ms at VIL and JAU substations were verified, respectively, resulting in an average reduction of the protection operation time of about 17 ms at both line terminals.

As a conclusion on the TD32 and TD21 elements, it is noticed that they are able to reduce the protection operation time in relation to the actual relays installed in the evaluated line, even without the support of the TW32 and TW87 elements. Also, from the studied cases, it is observed that the overcurrent supervision elements do not compromise the relay high-speed operation, although they have some influence on the final relay tripping time, which can be in turn further accelerated by using the traveling wave-based elements.

B. Part 2: TD32, TD21, TW32 and TW87 Evaluation Using Simulated Fault Records

In this evaluation stage, the SEL-T400L operation when both incremental quantity- and traveling wave-based elements operate together was evaluated using simulated records. Indeed, when detectable traveling waves are launched on the monitored line, the TW32 and TW87 can further accelerate the TD21 and TD32 operations, in such a way that operation times in the order of very few milliseconds may be verified.

Table IV depicts the obtained results for seven simulated fault cases, in which the fault type and location were varied. Since this evaluation part is focused on the study of the combined operation of both incremental quantity- and traveling wave-based protection elements, the communication link latency was not accounted for in the obtained results. Besides, only solid faults initiated at the voltage peak were considered, which are typical features of adverse short-circuits cases, during which the traveling wave-based elements are expected to operate [3].

TABLE II
PH21, PH87, TD32 AND TD21 EVALUATION USING REAL-WORLD FAULT RECORDS.

Real Case Number	Fault type/ location from VIL (pu)	Phasor-Based Relay Operation Time (ms)		Time-Domain Relay Operation Time (ms)	
		VIL	JAU	VIL	JAU
		PH21 / PH87	PH21 / PH87	(TD21 / OC21) ǀ (TD32 / OCTP)	(TD21 / OC21) ǀ (TD32 / OCTP)
R1	Internal BG / 0.46	●19.3 / ●30.0	●19.1 / ●32.2	(●5.5 / ●0.8) ǀ (●1.6 / ●1.4)	(●6.5 / ●0.7) ǀ (●2.3 / ●5.5)
R2	Internal CA / 0.46	●25.5 / ●29.8	●22.3 / ●28.4	(●9.8 / ●1.4) ǀ (●0.7 / ●1.4)	(●9.8 / ●1.3) ǀ (●0.7 / ●1.9)
R3	Internal BG / 0.08	●17.0 / ●27.3	○ / ●25.2	(●1.9 / ●0.6) ǀ (●0.7 / ●0.9)	(○ / ●1.0) ǀ (●2.4 / ●2.0)
R4	Internal CG / 0.06	●19.8 / ●25.1	○ / ●25.6	(●1.2 / ●0.4) ǀ (●0.7 / ●0.6)	(○ / ●0.7) ǀ (●0.7 / ●1.4)
R5	Internal BG / 0.63	●24.5 / ●29.7	●18.4 / ●28.4	(○ / ●0.6) ǀ (●0.7 / ●1.0)	(●2.2 / ●0.6) ǀ (●0.7 / ●1.1)
R6	Internal CG / 0.14	●20.0 / ●26.8	○ / ●25.5	(●1.2 / ●0.5) ǀ (●0.7 / ●0.7)	(○ / ●0.7) ǀ (●0.7 / ●1.4)
R7	Internal BG / 0.044	●18.5 / ●27.8	○ / ●27.4	(●4.7 / ●0.6) ǀ (●0.7 / ●0.9)	(○ / ●1.3) ǀ (●1.6 / ●2.8)
R8	External BG	○ / ○	○ / ○	(○ / ○) ǀ (○ / ○)	(○ / ●1.0) ǀ (●0.7 / ○)

Legend: ● = Operation / ○ = No operation.

TABLE III
TIME-DOMAIN RELAY OPERATION TIMES CONSIDERING POTT AND DTT SCHEMES IN INTERNAL FAULT CASES.

Real Case	VIL Substation (ms)			JAU Substation (ms)		
	TD21 & OC21	DTT	POTT	TD21 & OC21	DTT	POTT
R1	5.5	5.5	9.5	6.5	6.5	5.6
R2	9.8	9.8	5.9	9.8	9.8	5.4
R3	1.9	1.9	6.4	○	5.9	4.9
R4	1.2	1.2	5.4	○	5.2	4.7
R5	0.6	0.6	5.1	2.2	2.2	5.0
R6	1.2	1.2	5.4	○	5.2	4.7
R7	4.7	4.7	6.8	○	8.7	4.9

Legend: ○ = No operation.

From Table IV, it can be observed that SEL-T400L time-domain elements were even faster than in the previously analyzed real-world fault cases. In all internal and external fault scenarios, the SEL-T400L relay operation occurred as expected, resulting in operation times that did not exceed the order of 7.8 ms. It can be seen that the TD21 and TD32 operation occurred in few milliseconds only, as expected, whereas the TW32 and TW87 resulted in operation times below 1.9 ms.

With respect to the TD21 function combined with the OC21 element, comparing cases S1, S2 and S3, one can see that the greater the fault distance the slower the protection operation. Also, in case S4, in which a fault at the TD21 reaching point is simulated, no operation was verified in VIL substation, but the fault was detected in JAU substation 1.8 ms after the fault inception. Indeed, the TD21 is expected to underreach in some cases, depending on the system transients soon after the fault inception [3]. However, by using a DTT scheme, such a problem could be overcome, guaranteeing a fast and reliable transmission line tripping.

Regarding the TD32 combined with the OCTP and TW32 elements, correct operations were verified in all simulations, properly indicating the fault direction even in cases of faults at the monitored buses (cases S6 and S7). In case S5 (external fault at the parallel circuit), the TD32 element at JAU substation indicated a forward fault, since part of the fault contribution flowed through the circuit C1 from JAU toward VIL substation. Even with this operation, the POTT scheme restrained, because the elements at VIL substation did not issued the permissive trip. Besides, regarding the TW32, it should be pointed out that such a function resulted in ultra-high-speed operations, detecting the fault direction in less than 0.1 ms, speeding up the POTT scheme in cases S1, S2, S3 and S4. As a result, tripping times smaller than those verified in the previous section (where only the TD21 and TD32 schemes were considered) would be verified. Furthermore, in the evaluated external fault cases S5, S6 and S7, the TW32 properly indicated reverse faults at the terminals closer to the simulated faults, guaranteeing the protection security.

In relation to the TW87, it is noticed that it properly distinguished internal from external fault cases in all simulated scenarios, attesting its reliability and security. Besides, the OC87 element did not delay the TW87 operation in the evaluated internal fault scenarios. Hence, assuming that a reliable traveling wave detection is performed at both line ends, one can conclude that the TW87 operation time depends mainly on the communication link delay and line length. Even so, for the evaluated line, for which a link delay of about 4 ms is realistic, the TW87 operation times would not exceed the order of 6 ms in the analyzed fault scenarios, which is much less than the operation times typically obtained via phasor-based elements.

TABLE IV
TD32, TD21, TW32 AND TW87 EVALUATION USING SIMULATED FAULT RECORDS.

Simulated Case Number	Fault type/ location from VIL (pu)	Substation	Time-Domain Relay Operation Time (ms) (TD21 / OC21) | (TD32 / TW32 / OCTP) | (TW87 / OC87)
S1	Internal AB / 0.5	VIL	(●7.8 / ●0.5) | (●0.7 / ●<0.1 / ●0.5) | (●0.7 / ●0.5)
		JAU	(○ / ●0.5) | (●0.7 / ●<0.1 / ●1.2) | (●1.2 / ●1.2)
S2	Internal AT / 0.05	VIL	(●1.2 / ●0.3) | (●0.7 / ●<0.1 / ●0.5) | (●1.9 / ●0.5)
		JAU	(○ / ●0.6) | (●0.7 / ●<0.1 / ●1.1) | (●1.1 / ●1.1)
S3	Internal AT / 0.30	VIL	(●1.6 / ●0.4) | (●0.7 / ●<0.1 / ●0.7) | (●1.2 /●0.7)
		JAU	(○ / ●0.5) | (●0.7 / ●<0.1 / ●1.0) | (●1.0 / ●1.0)
S4	Internal AT / 0.70	VIL	(○ / ●0.5) | (●0.7 / ●<0.1 / ●0.8) | (●0.8 / ●0.8)
		JAU	(●1.8 / ●0.4) | (●0.7 / ●<0.1 / ●0.9) | (●1.3 / ●0.9)
S5	External AT / 0.5 (in Circuit C2)	VIL	(○ / ○) | (○ / ○ / ○) | (○ / ●8.0)
		JAU	(○ / ●0.7) | (●0.7 / ○ / ●12.6) | (○ / ●12.1)
S6	External AT / 1.0 at JAU	VIL	(○ / ●0.9) | (●0.7 / ●<0.1 / ●1.5) | (○ / ●1.5)
		JAU	(○ / ○) | (○ / ○ / ○) | (○ / ●2.1)
S7	External AT / 0.0 at VIL	VIL	(○ / ○) | (○ / ○ / ○) | (○ / ●1.2)
		JAU	(○ / ●0.6) | (●0.7 / ●<0.1 / ●1.2) | (○ / ●1.2)

Legend: ● = Operation / ○ = No operation / < 0.1 = Smaller than 0.1 ms.

Still regarding Table IV, it is observed that the time-domain elements performed well even in cases of faults at the monitored buses, i.e., at VIL and JAU substations (see cases S6 and S7). Also, faults in the parallel circuit C2 did not result in a false trip (see case S5), restraining the trip, as expected. It demonstrates that the time-domain protection elements available in the SEL-T400L relay are promising for the evaluated test power system, since they resulted in an average operation time reduction in the order of one power cycle in internal fault cases in relation to the phasor-based relays installed in the line, without resulting in false trips during external fault disturbances.

V. CONCLUSION

In this paper, a performance analysis of actual time-domain SEL-T400L relays considering Brazilian fault cases was presented. The obtained results clarify questions that have been reported by Brazilian utilities on the performances of the TD32, TD21 TW32 and TW87 time-domain elements.

A Brazilian 230 kV/60 Hz line with high number of outages per year was analyzed by means of real-world and simulated fault records. During the analysis of real-world cases, due to sampling rate limitations, only the TD32 and TD21 functions were evaluated. Then, all SEL-T400L relay functions (TD32, TD21, TW32 and TW87) combined with their respective overcurrent supervision elements were tested by means of ATP simulated records. The obtained results show the SEL-T400L is promising for the evaluated transmission line. Indeed, it proved to be secure and reliable, reducing the protection operation times of about a power cycle in relation to the currently installed phasor-based relays.

ACKNOWLEDGMENT

The authors would like to thank the Brazilian National Council for Scientific and Technological Development (CNPq) and the Coordination for the Improvement of Higher Education Personnel (CAPES) for the finantial support, and Eletronorte and ONS for the technical support.

REFERENCES

[1] P. M. Anderson, *Power System Control and Stability*. Piscataway, NJ - USA: Wiley-IEEE Press, 2nd ed., 2003.

[2] *Ultra-High-Speed Transmission Line Relay Traveling-Wave Fault Locator High-Resolution Event Recorder*, Schweitzer Engineering Laboratories, 2018. [Online]. Available: https://selinc.com/products/T400L/

[3] E. O. Schweitzer, B. Kasztenny, and M. V. Mynam, "Performance of time-domain line protection elements on real-world faults," in *42nd Annual Western Protective Relay Conference*, Oct. 2015.

[4] J. P. G. Ribeiro and F. V. Lopes, "Modeling and simulation of a time-domain line protection relay," *IET Journals - The Journal of Engineering*, vol. 2018, no. 15, pp. 861–865, October 2018.

[5] F. V. Lopes, J. P. G. Ribeiro, E. J. S. Leite Jr., and K. M. Silva, "Parametric analysis of the travelling wave-based differential protection tw87," *IET Journals - The Journal of Engineering*, vol. 2018, no. 15, pp. 1297–1302, October 2018.

[6] E. Schweitzer, B. Kasztenny, A. Guzmán, V. Skendzic, and M. Mynam, "Speed of line protection - can we break free of phasor limitations?" in *68th Annual Conference for Protective Relay Engineers*, March 2015.

[7] B. Kasztenny, A. Guzmán, N. Fischer, M. V. Mynam, and D. Taylor, "Practical setting considerations for protective relays that use incremental quantities and traveling waves," in *43rd Annual Western Protective Relay Conference*, Oct 2016.

[8] *Doble Protection Testing F6150sv - Power System Simulator*, Doble Engineering Company, 2018.

[9] A. Guzman, Z. Sheffield, and D. Taylor, "Testing traveling-wave line protection and fault locators," in *14th International Conference on Developments in Power System Protection*, 2018.